JOURNAL OF MATERIALS SCIENCE 13 (1978) 261–267

Ionic conductivity and crystal structure of magnesium- and cobalt-doped sodium-beta-alumina

G. J. MAY
Chloride Silent Power Limited, Runcorn, Cheshire UK

The effect of cobalt as a dopant for sodium-beta-alumina has been studied in polycrystalline materials prepared from a mixed oxide precursor. Two materials have been examined; one containing a small amount of cobalt as well as magnesium as a dopant and the other magnesium alone to produce the same molar quality of divalent dopant. The sintering behaviour, microstructure and phase composition are shown to be related to the measured ionic conductivity.

1. Introduction

Fast ionic conduction in solids has attracted considerable research interest in recent years [1, 2] focussed particularly on sodium transport in sodium-beta-alumina because of its potential application as the electrolyte and separator in sodium–sulphur cells [3, 4]. The crystal structure of beta-alumina was first determined by Bragg [5] and by Beevers and Ross [6] who showed the material consisted of blocks of four close-packed layers of oxygen ions with aluminium ions in the interstices in the same positions as a spinel. These layers, referred to as spinel blocks, are bonded together by oxygen bridges and sodium ions (Fig. 1). The sodium ions are free to migrate in an electric field in these loosely packed planes. The two principal forms of beta-alumina are β- (hexagonal; $P6_3/mmc$; $a_0 = 0.559\,nm$, $c_0 = 2.261\,nm$) and β''-(rhombohedral; $R\bar{3}m$; $a_0 = 0.560\,nm$, $c_0 = 3.395\,nm$) which differ in the stacking sequence of the spinel blocks and the site occupancy of sodium in the layer planes [7, 8]. There are three possible sites for sodium in the sodium–oxygen layer consistent with the space group $P6_3/mmc$, $2d$, $2c$ and $6h$, and it was shown by Beevers and Ross that sodium occupied the $2d$ site. These positions are referred to as the BR (Beevers–Ross), aBR (anti-Beevers–Ross), and mO (mid-oxygen) sites, respectively. A later and more refined structural determination by Peters *et al* [9] confirmed the structure found by Beevers and Ross but found that the sodium did

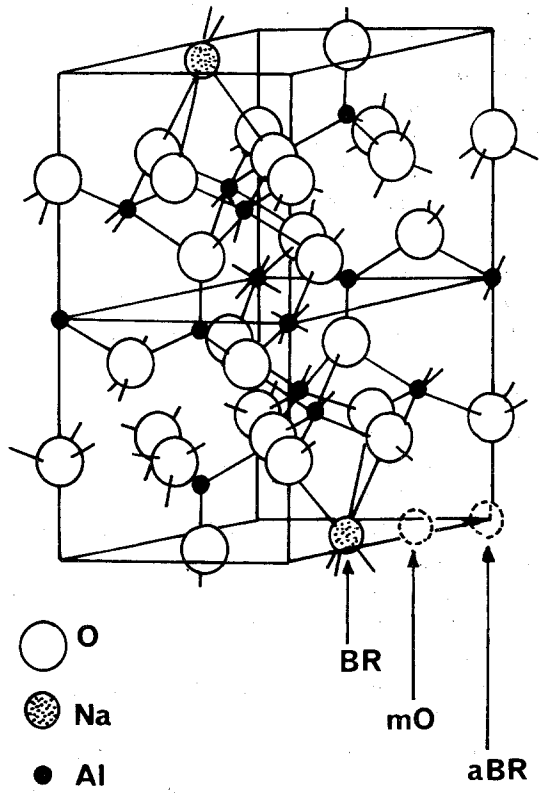

Figure 1 Crystal structure of beta-alumina. The diagram shows a single spinel block, i.e., half the unit cell. Sodium is shown in the Beevers–Ross (BR) site and the dotted circles show the alternative mid-oxygen (mO) and anti-Beevers–Ross (aBR) positions.

not simply occupy BR sites and was distributed in a triangular pattern with three-quarters of the sodium density close to the BR position and the remainder in the mO position. The aBR position was empty. This disorder accounts for the rapid diffusion in the basal plane as sodium ions can readily exchange positions between occupied and vacant sites. There is an excess of sodium ions in β-alumina and there has been speculation as to whether the charge compensating defects required to preserve electrical neutrality were aluminium vacancies or oxygen interstitials. Recently, however, Roth *et al* [10] have identified a compound defect as a result of neutron diffraction studies which has the formula,

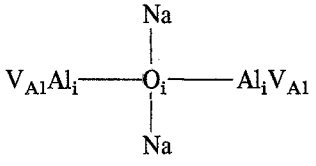

where $V_{Al}Al_i$ is a Frenkel defect (an aluminium vacancy–interstitial pair) and O_i an interstitial oxygen ion in the mO positon in the conduction plane. β''-alumina tends to be more conductive than β-alumina and is stabilized by a variety of dopants that substitute for aluminium ions in the spinel blocks. Roth *et al* have shown that the compound defects observed in β-alumina were not present in β''-alumina and that the spinel blocks were essentially free of vacancies and interstitial aluminium ions. Most published work has been concerned with magnesium- and lithium-doped materials and only a few workers have studied other doping ions. This paper reports on examination of the effect on the ionic conductivity and sintering behaviour of combining a small amount of cobalt with magnesium as dopants.

Kennedy and Akridge [11] have investigated the sintering characteristics and resistivity of β-alumina doped with vanadium, chromium, magnesium, iron, nickel or cobalt. All of these dopants inhibited the sintering behaviour of β-alumina to a certain extent and vanadium (added as V_2O_5) acted as a very effective sintering inhibitor. The cobalt-doped material (2 wt%) had a room temperature ionic resistivity of 6.3 Ωm, which may be compared with a value of 18 Ωm for undoped material. The ionic resistivity of beta-alumina doped with magnesium, nickel, zinc, copper and calcium respectively was measured by Imai and Harata [12]. They found that magnesium and zinc were especially effective in decreasing the ionic resistivity and that copper and nickel also produced decreases in resistivity, but that calcium-doped material had a poor resistivity. This was confirmed by De Jonghe and Hsieh [13] who have also examined the effect of silicon on the resistivity of beta-alumina. Calcium and silicon do not substitute for aluminium ions in the spinel block but form discrete intergranular phases that substantially increase the ionic resistivity. A detailed crystal structure determination of cobalt-doped potassium-β-alumina has been carried out by Dernier and Remeika [14]. The cobalt-doped material was isomorphous with pure, un-doped material and they showed that the cobalt ions selectively occupied tetrahedral sites in the spinel blocks. Comparison of bond lengths between doped and un-doped material suggested that charge compensation was achieved by means of aluminium vacancies, although the data are not inconsistent with the compound defects proposed by Roth and co-workers.

In this work the effect of adding a small amount of cobalt to a magnesium-doped sodium-beta-alumina has been studied. Polycrystalline ceramic tubes have been prepared containing magnesium oxide as a dopant and with a mixture of a small amount of cobalt oxide and magnesium oxide to produce the same molar quantity of dopant. The ionic resistivity of the two materials has been compared and the sintering behaviour and micromorphology are described.

2. Experimental

Beta-alumina samples were prepared in the form of thin-walled, closed-ended tubes, 33 mm outside diameter by 225 mm long with a wall thickness of 1.5 mm from two compositions: (a) 8.0 wt% Na_2O, 2.0 wt% MgO, balance Al_2O_3; (b) 8.0 wt% Na_2O, 1.80 wt% MgO, 0.37 wt% CoO, balance Al_2O_3. The relative amounts of magnesium oxide and cobalt oxide in composition (b) provide the same molar quantity of divalent dopant as in composition (a). Both materials were made up from high purity starting materials in the form of finely ground α-alumina, magnesium oxide, sodium aluminate and, in the case of the cobalt-doped material, cobalt nitrate. These were dry vibro-energy milled together using α-alumina cylinders as grinding media to produce a homogeneous mixture, and green shapes were produced by isotatic pressing with a pressure of 275 N mm^{-2}. These

samples were then fired in a rapid, pass-through zone-sintering furnace with a peak temperature of 1975 K and a relatively short hot-zone length a range of speeds from 40 to 60 mm min^{-1}. The atmosphere in the firing zone was oxidizing and saturated with sodium oxide vapour. The short, buffered firing cycle minimized the sodium oxide loss by evaporation and so the final composition was close to the green body. This was confirmed by X-ray fluorescence analysis of the sintered material. Sintered densities were measured by a simple Archimedean technique.

The relative proportions of β- and β''-alumina were determined by measurements of the relative peak heights of selected reflections on an X-ray diffractometer trace. The d-spacings were calculated and, correctly indexed, were used to calculate accurate lattice parameters for both phases using the Nelson–Taylor–Riley–Sinclair extrapolation function to compensate for geometric errors. The microstructure was examined by optical microscopy after grinding with silicon carbide paper, polishing with 1 μm diamond paste and etching in boiling phosphoric acid for 3 min. The microstructure was also studied directly by examination of fracture surfaces in an ISI Mini-SEM scanning electron microscope.

The ionic resistivity was measured using a simple d.c. four-probe method [15]. Four silver wires were wrapped around the tube and each wire was wetted with a small amount of an aqueous solution of sodium nitrite and sodium nitrate in eutectic proportions (Fig. 2). A small current was passed between the outer probes in both directions and the potential between the inner probes measured. Care was taken to eliminate effects due to electrode polarization, to slight differences in the composition of the sodium nitrate/nitrite eutectic, or to slight compositional differences in the ceramic sample. The ionic resistivity was calculated directly from the measured resistance and dimensions of the sample.

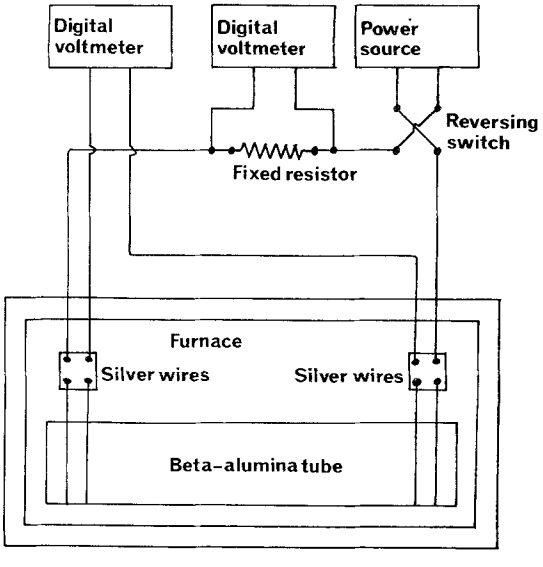

Figure 2 Schematic diagram of 4-terminal d.c. conductivity measuring equipment.

3. Results and discussion

The magnesium-doped material (a) had a sintered density of 3240 kg m^{-3} (99% theoretical density) and a high degree of translucency. The cobalt-containing material (b) had an intense, uniform blue coloration but had a slightly lower density, 3170 kg m^{-3} (97% theoretical density). The presence of small amounts of cobalt evidently inhibits densification as noted by Kennedy and Akridge [11].

Microscopic examination of sample (b) before etching showed rounded pores ranging in size from approximately 1 μm to 15 μm in diameter. Visual estimation revealed a fairly even distribution of pores within this size range and many of the small pores appeared to be associated with larger grains. Etching revealed a duplex grain structure with larger lath-shaped grains in a fine matrix (Fig. 3). The size of the lath shaped sections varied from about 7 μm x 35 μm to 25 μm x 180 μm. The matrix was difficult to resolve optically, the apparent grain size being less than 1 μm, and this was confirmed by direct examinationin the scanning electron microscope. The distribution of cobalt as evidenced by the depth of the blue colouration was very uniform on a macroscopic scale but some colour differences were seen under the microscope, although this could be caused by scattering of light by pores and by grains of different sizes. The uniformity was confirmed by energy dispersive analysis of X-rays in the scanning electron microscope which showed no significant difference in the counting rate for the principal cobalt peak at different points. The magnesium-doped material had rounded pores in the sizes range 2 to 12 μm with the majority in the range 3 to 6 μm. The material had a duplex micromorphology with a fine-grained matrix (grain sizes in the range 0.5 to 2.0 μm) but only a few larger lath-shaped grains with a maximum length of 50 μm (Fig. 4).

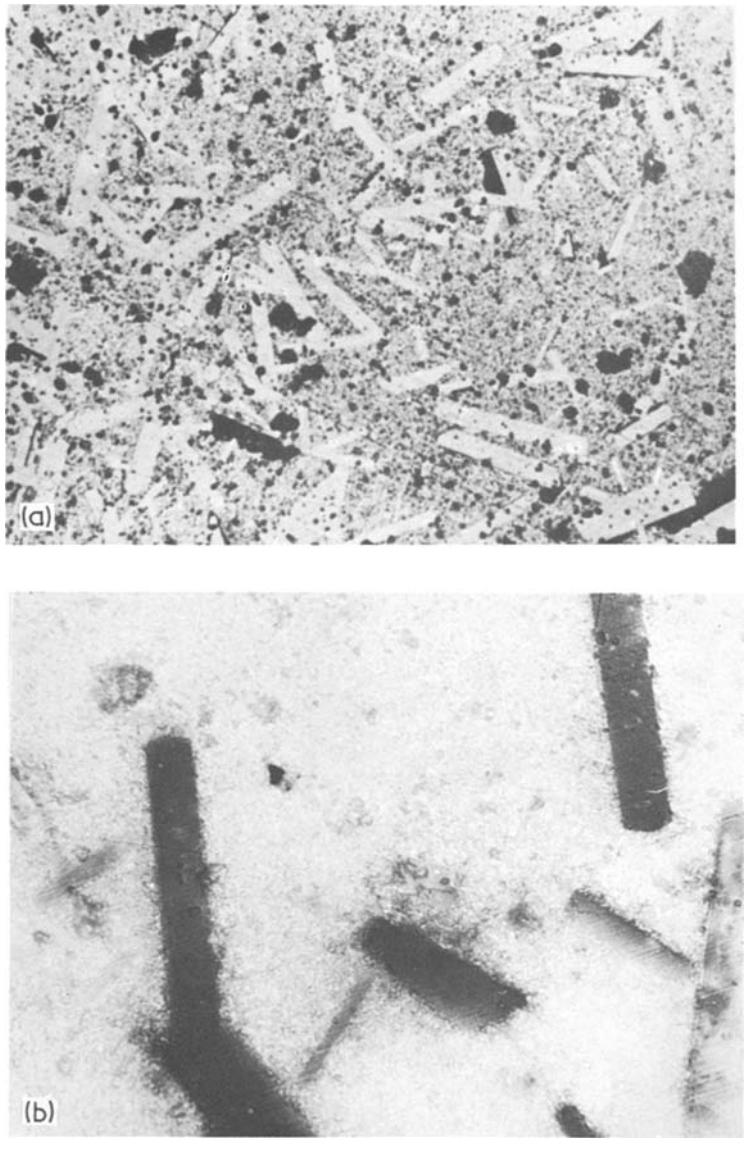

Figure 3 Microstructure of cobalt and coarse grains in a fine-grained matrix, (a) magnesium doped beta-alumina showing X 120, (b) X 600.

The higher porosity of the cobalt-containing material was partly due to the larger proportion of coarse grains, as these tended to contain a relatively large pore volume. Fig. 5 shows scanning electron micrographs of the fracture surface showing large grains in the fine-grained matrix with large rounded pores within these grains. Diffusion of trapped gases out of the pores and of solid material into pores is clearly more sluggish within a relatively massive beta-alumina grain than in the fine-grained matrix because of the larger pore–boundary distances.

The relative proportions of the β- and β''-phases were estimated from the heights of the $(0\,1\,\bar{1}\,2)$, $(0\,1\,\bar{1}\,3)$ β- and $(0\,1\,\bar{1}\,2)$, $(1\,0\,\bar{1}\,4)$ β''-peaks and from the $(0\,2\,\bar{2}\,6)$, $(0\,2\,\bar{2}\,7)$ β- and $(0\,2\,\bar{2}\,1\,0)$ β''-peaks. The volume fraction of the β-phase was approximately 0.5 in both materials. Accurate values of the lattice constants and their standard deviations were calculated from lattice parameters derived from individual d-spacings by a least squares analysis of these data, suitably weighted to favour high angle lines, using the Nelson–Riley–Taylor–Sinclair function. The values are given

Figure 4 Microstructure of magnesium-doped beta-alumina showing fine grain structure and substantial absence of coarse grains, × 750

below:

$$
\begin{aligned}
\text{(a)}\ \beta\text{-};\ a_0 &= 0.5609 \pm 0.0004\ \text{nm},\\
c_0 &= 2.235 \pm 0.002\ \text{nm}.\\
\beta''\text{-};\ a_0 &= 0.5607 \pm 0.0003\ \text{nm},\\
c_0 &= 3.365 \pm 0.005\ \text{nm}.\\
\text{(b)}\ \beta\text{-};\ a_0 &= 0.5604 \pm 0.0005\ \text{nm},\\
c_0 &= 2.252 \pm 0.004\ \text{nm}.\\
\beta''\text{-};\ a_0 &= 0.5595 \pm 0.0005\ \text{nm},\\
c_0 &= 3.396 \pm 0.007\ \text{nm}.
\end{aligned}
$$

Both materials have approximately equal a_0 parameters which is consistent with β- and β''-alumina existing as a mixed intergrowth structure [16, 17] with lattice matching on the basal plane. Comparing the c_0 parameters of the β- and β''-structure of the two materials shows the same change ((a), 50.6%; (b), 50.8%) but a comparison of the c_0 parameters for each phase shows a significant increase for the cobalt-doped material. The β-c_0 value was increased by 0.8% and the β''-c_0 value by 0.9%. Evidently the cobalt does not partition preferentially to one of the phases and it may be inferred that if cobalt ions substitute for aluminium ions in the spinel blocks in the same positions as magnesium ions, the equal distribution of cobalt between the phases implies an equal distribution of magnesium between β- and β''-alumina. The change in lattice parameter is expected if divalent cobalt ions are substituted in the same positions as magnesium ions since the ionic radius of divalent cobalt is 0.072 nm, whereas the ionic

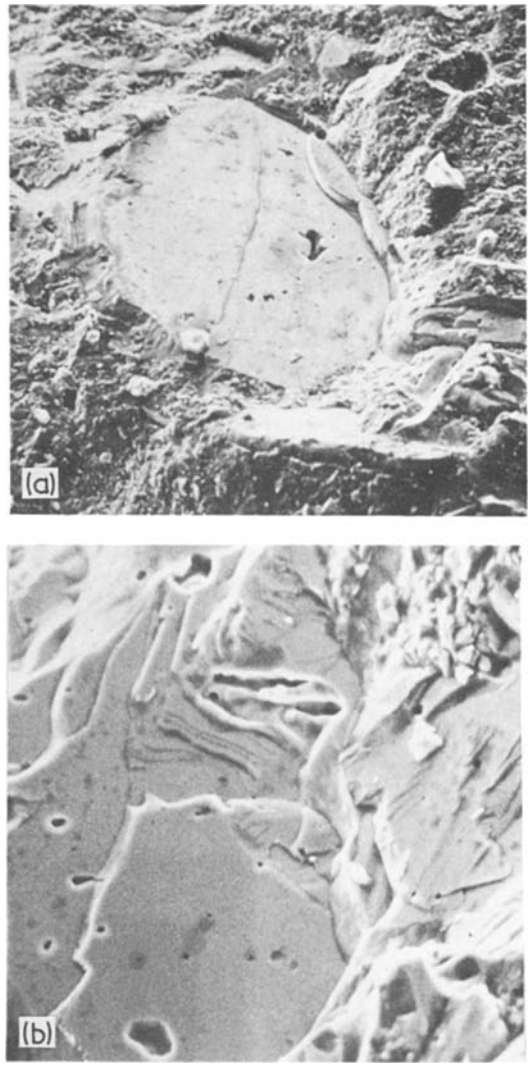

Figure 5 Scanning electron micrographs of fracture surfaces of cobalt-containing material shown cleavage facets of large grains in a fine-grained matrix with trapped closed pores in the large grains, (a) × 400, (b) × 1600.

radius of magnesium is 0.065 nm. If cobalt were present as Co^{3+}, a small contraction in the c_0 value would be observed, as the ionic radius is 0.063 nm. It can be concluded that the cobalt is present as Co^{2+} and that cobalt behaves in a similar manner to magnesium in beta-alumina.

The ionic conductivity σ follows an Arrhenius relation of the form,

$$\sigma = (\sigma_0/T) \exp -(E_a/RT)$$

where σ_0 is a constant, T is the absolute temperature, E_a the activation energy for ionic motion and R the gas constant. The results are plotted in Fig.

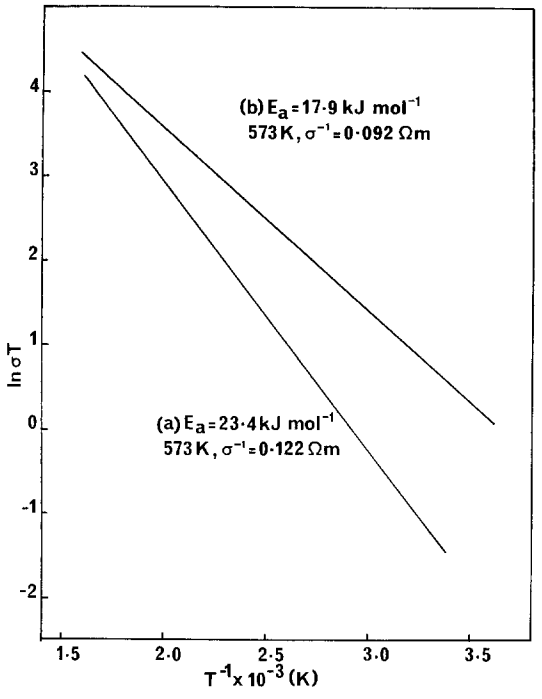

Figure 6 Graph of ln σT against reciprocal temperature for magnesium-doped beta-alumina (a) and for magnesium and cobalt-doped beta-alumina (b).

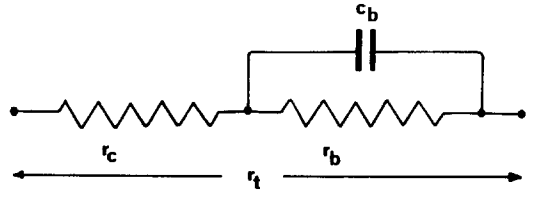

Figure 7 Equivalent circuit for polycrystalline beta-alumina.

6 as a graph of the logarithm of the product σT against reciprocal temperature and the activation energies are determined from the slope of the resulting straight line. The ionic resistivity of the cobalt-containing material at 573 K is 0.092 Ωm, and the ionic resistivity of the magnesium-doped material at the same temperature is 0.122 Ωm. The corresponding values for the activation energies measured between 550 and 675 K are 17.8 kJ mol^{-1} and 23.4 kJ mol^{-1}. This improvement in ionic conductivity is unexpected in view of the work of Kennedy and co-workers, who found that magnesium alone was more effective in improving the ionic conductivity [11, 18], and also in view of the similarity of the volume fractions of the β-phase between the two materials. The overall ionic resistivity r_t of beta-alumina is the sum of the resistivities of the grain bulk r_c and the grain boundaries r_b. There is also an associated grain boundary capacitance c_b (Fig. 7). The relatively high activation energy for magnesium-doped material is associated with a significant grain-boundary contribution to the overall resistivity which has been demonstrated by complex plane analysis of a.c. conductivity measurements over a range of frequencies from 500 Hz to 2 MHz [19]. These measurements allow the grain-boundary and grain-bulk resistivities to be separated and in Arrhenius plots for each component the activation energy associated with the grain boundaries was 23 kJ mol^{-1}, whereas the value for the grain bulk was 14 kJ mol^{-1}. The same trend in the relative values of grain-boundary and grain-bulk activation energies of polycrystalline beta-alumina doped with magnesium, zirconium and yttrium was found by Powers and Mitoff [20] who found a grain-boundary value of 28 kJ mol^{-1} and a grain-bulk value of 18 kJ mol^{-1}. Furthermore it has been shown that in magnesium-doped beta-alumina with the same composition as (a) but a larger, uniform grain size in the range 30 to 40 μm the grain-boundary contribution to the overall resistivity was substantially reduced [21]. An alternative explanation for the improved conductivity of the cobalt-doped material is that the cobalt is conferring some electronic conductivity, but this is not the case as both materials show the full open-circuit voltage in sodium–sulphur cells. Consequently the decrease in activation energy and resistivity are probably the result of the increase in average grain size due to the substantial proportion of coarse grains.

4. Conclusions

Polycrystalline beta-alumina tubes have been prepared from mixed oxide precursors containing magnesium oxide and a mixture of magnesium oxide and cobalt oxide to produce the same molar quantity of divalent dopant. The addition of cobalt oxide reduced the sintered density of the material and increased the volume fraction of coarse grains in the fine-grained matrix. There was no change in the relative proportions of β- and β″-alumina. A small change in the lattice parameter (c_0) for both the β- and β″-phases was consistent with the substitution of divalent cobalt ions in the spinel blocks of the beta-alumina lattice. The ionic resistivity of the cobalt-containing material was lower than that of the magnesium-doped material

as a result of the increased volume fraction of coarse grains.

Acknowledgements

The assistance of Sheila Ruddlesden and Stephen Tan is gratefully acknowledged. This paper is published by permission of Chloride Silent Power Limited.

References

1. P. W. McGEEHIN and A. HOOPER, *J. Mater. Sci.* **12** (1977) 1.
2. J. T. KUMMER, *Prog. Solid State Chem.* 7 (1972) 141.
3. N. WEBER and J. T. KUMMER, *Adv. Energy Conv. Eng.*, ASME Conference, Florida (1967) p. 913.
4. G. J. MAY and I. W. JONES, *The Metallurgist and Materials Technologist* 8 (1976) 427.
5. W. L. BRAGG, C. GOTTFRIED and J. WEST, *Z. Krist.* 77 (1931) 255.
6. C. A. BEEVERS and M. A. S. ROSS, *ibid* 97 (1937) 59.
7. Y. YAMAGUCHI and K. SUZUKI, *Bull. Chem. Soc. Japan* **41** (1968) 93.
8. M. BETTMAN and C. R. PETERS, *J. Phys. Chem.* 73 (1969) 1774.
9. C. R. PETERS, M. BETTMAN, and J. W. MOORE and M. P. GLICK, *Acta Cryst.* **B27** (1971) 1826.
10. W. L. ROTH, F. REIDINGER and S. LaPLACA, "Superionic Conductors", edited by G. D. Mahon and W. L. Roth (Plenum Press, New York (1976) p. 223.
11. J. H. KENNEDY and J. R. AKRIDGE, *J. Am. Ceram. Soc.* **58** (1976) 279.
12. A. IMAI and M. HARATA, *Jap. J. Appl. Phys.* **11** (1972) 180.
13. L. C. DE JONGHE and M. Y. HSIEH, Proceedings of the Symposium and Workshop on Advanced Battery Research, March 1976, Argonne National Laboratory, B13.
14. P. D. DERNIER and J. P. REMEIKA, *J. Solid State. Chem.* **17** (1976) 245.
15. L. J. MILES and I. W. JONES, *Proc. Brit. Ceram. Soc.* **19** (1969) 161.
16. D. J. M. BEVAN, D. HUDSON and P. T. MOSELEY, *Mater. Res. Bull.* 9 (1974) 1073.
17. H. SATO and Y. HIROTSU, *ibid.* **11** (1976) 1307.
18. J. H. KENNEDY and A. F. SAMMELLS, *J. Electrochem. Soc.* **119** (1972) 1609.
19. A. HOOPER, personal communication.
20. R. W. POWERS and S. P. MITOFF, *J. Electrochem. Soc.* **122** (1975) 226.
21. G. J. MAY, Unpublished research.

Received 15 April and accepted 5 July 1977.